

This article was downloaded by:

On: 17 January 2011

Access details: *Access Details: Free Access*

Publisher *Taylor & Francis*

Informa Ltd Registered in England and Wales Registered Number: 1072954 Registered office: Mortimer House, 37-41 Mortimer Street, London W1T 3JH, UK



Critical Reviews in Analytical Chemistry

Publication details, including instructions for authors and subscription information:

<http://www.informaworld.com/smpp/title~content=t713400837>

CLAY MINERALS AND HEAVY METALS

Edward H. Smith; Tomas Vengris

Online publication date: 03 June 2010

To cite this Article Smith, Edward H. and Vengris, Tomas(1998) 'CLAY MINERALS AND HEAVY METALS', Critical Reviews in Analytical Chemistry, 28: 2, 13 – 18

To link to this Article: DOI: 10.1080/10408349891194225

URL: <http://dx.doi.org/10.1080/10408349891194225>

PLEASE SCROLL DOWN FOR ARTICLE

Full terms and conditions of use: <http://www.informaworld.com/terms-and-conditions-of-access.pdf>

This article may be used for research, teaching and private study purposes. Any substantial or systematic reproduction, re-distribution, re-selling, loan or sub-licensing, systematic supply or distribution in any form to anyone is expressly forbidden.

The publisher does not give any warranty express or implied or make any representation that the contents will be complete or accurate or up to date. The accuracy of any instructions, formulae and drug doses should be independently verified with primary sources. The publisher shall not be liable for any loss, actions, claims, proceedings, demand or costs or damages whatsoever or howsoever caused arising directly or indirectly in connection with or arising out of the use of this material.

CLAY MINERALS AND HEAVY METALS

EDWARD H. SMITH and TOMAS VENGRIS

Environmental Engineering Program, Southern Methodist University, Institute of Chemistry

Introduction

Heavy metals, deriving from industrial wastewater discharges, present an ongoing and serious threat to human health and natural water quality. Due to their abundance near the surface, naturally occurring phyllosilicate clay minerals play an important role in regulating the fate and transport of heavy metals in subsurface waters. In developing areas such as Eastern Europe, some of these minerals may also serve as cost-effective sorbents for the removal of heavy metals within the economic constraints of the region. While their sorption capacities are generally less than those of commercial adsorbents, these materials could provide an inexpensive substitute for pre- or post-treatment of heavy metal wastewaters. For instance, substantial glauconite deposits are present in the Baltic region and other parts of Eastern Europe, with several hundred million tonnes reportedly accessible in Lithuania [1]. Recent experimental and modeling studies have demonstrated that: (1) Lithuanian glauconite has a heavy metal adsorbing capacity comparable to and, in some instances, greater than that of other oxide-coated clayey minerals; and, (2) surface complexation models are a useful tool for understanding hydrous surface properties of complex clay minerals such as glauconite and characterizing their sorptive interactions with heavy metals [1-2]. The primary aim of this work is to present the results of ongoing studies on the sorption of heavy metals by Lithuanian glauconite and other locally-available clayey materials.

Experimental Methods

Materials. Samples of a lower Cretaceous glauconite deposit were taken from the Jonava region of central Lithuania. Glauconite belongs to the mica (dioctahedral) group, with enriched Fe, more than 0.4 Al per 8 Si of tetrahedral substitution and more than 2.4 atoms per four sites of octahedral R^{3+} [3-4]. It has a three-layer sheet structure with 2:1 layer type (1 octahedral and 2 tetrahedral layer) alternating with a layer of water molecules and alkaline metal elements, mostly potassium. The mineral and chemical compositions of the sample were determined by electron microprobe analysis, averaging almost ninety percent pure glauconite with minor quartz, k-feldspar, garnet, rutile, sillenite, ilmenite, and hornblende. Glauconite samples were used *as is* in adsorption experiments except for sieving into various particle size fractions and washing with deionized, distilled water. Some comparative tests were performed with two other locally-available, natural clay samples, referred to here as NR-1 and NR-2. NR-1, from Shaltishkiai deposit, has a mineralogical composition of 50-55% hydromica, 30-35% montmorillonite, and 10-15% chlorite. The total clay mineral content is estimated at 63.5%, with the remainder including quartz, mica, feldspar, *etc.* NR-2 was obtained from the Daugeliai deposit and is 80-85% hydromica, 5-10% kaolinite, and 5-10% chlorite. The clay mineral content of NR-2 is 80.5%. For use as sorbents, NR-1 and NR-2 underwent thermal pretreatment at 700 °C for 0.5 hour.

Sorption Studies. Adsorption equilibrium studies were conducted in well-sealed, 125-mL teflon bottles which, when agitated, can be assumed to function as completely mixed batch reactors. A prescribed mass of sorbent was placed in a series of bottles containing 100 mL of aqueous solution at preestablished conditions of ionic strength and total dissolved metal concentration, C_0 . The pH of individual bottles was adjusted to achieve a range for the series of between 3.5 and 10.5. Following a 48-hour reaction period on a rotary tumbler, the

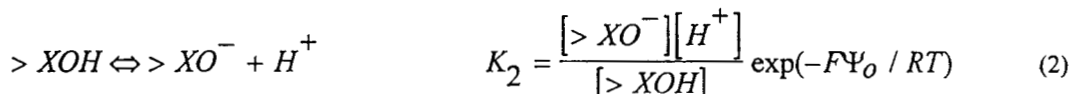
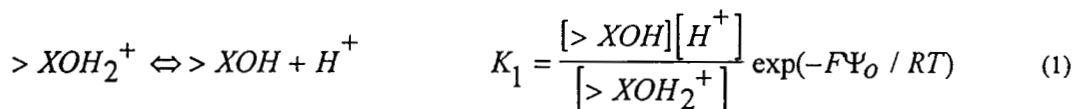
equilibrium pH was measured and a sample taken from each reactor and filtered to separate the solid. The aqueous samples were acidified with 3 N HClO₄ and analyzed for equilibrium liquid phase concentration of metal, C_e , using an inductively coupled plasma (ICP) spectrometer. Two or three reactors containing no sorbent were included to establish the total concentration of sorbate. Solid-phase loading of metal, Q_e , was then computed from a mass balance. A repeat experiment without glauconite provided observation of metal-solubility/precipitation phenomena for a particular solution-phase condition.

Column experiments were conducted in stainless steel columns with an internal diameter of either 0.48 cm or 0.78 cm. The columns were packed with successive layers of teflon flakes, sorbent, and teflon flakes between stainless steel mesh screens. Test solution containing the target metal(s) was pumped through the bed in upflow mode using an Eldex B high pressure pump at surface loadings of 4.9-9.8 m³/m²·hr. Effluent samples were collected at frequent intervals in polyethylene tubes, acidified, and analyzed for metals by ICP. A three-way valve prior to the inlet enabled collection of influent samples to confirm the feed concentration, C_0 .

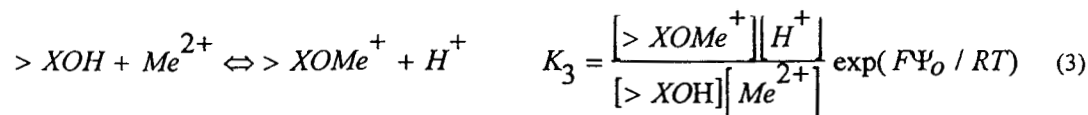
Cadmium, lead, zinc, and copper were the metals examined in the study. Working solutions were prepared from concentrated stock solutions of reagent grade metal salts. Total metal concentrations ranged from 0.5 to 50 ppm and ionic strength, I , varied from $I = 10^{-3}$ to 10^{-1} M as NaClO₄. pH adjustment was with either 1 N HClO₄ or 1 N NaOH under a nitrogen, CO₂-free atmosphere. ICP metal analysis employed four-point standard calibration prior to and following analysis of unknowns, and regular triplicate analyses to confirm the method.

Results and Discussion

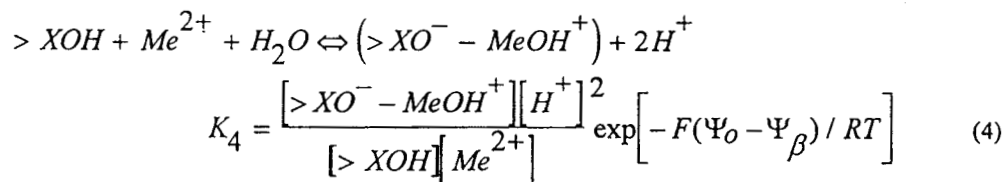
Adsorption capacity of heavy metals by Lithuanian glauconite was greatest for Pb followed in order by Cu, Cd, and Zn. Sorption equilibria were quantified in terms of a surface complexation approach as presented in Table 1. Surface complexation is assumed to be a primary mechanism for heavy metal removal onto complex clay sorbents. By virtue of their composition, these materials have oxide or hydroxylated surface sites in solution such as $>XOH_2^+$, $>XOH$, and XO^- representing positively charged, neutral, and negatively charged sites, respectively. The symbol, $>X$ represents the surface oxide base element, in this case, typically Si, Fe, Al, and possibly Mg. The aqueous phase equilibria associated with these surface groups can be written as:



In the exponential term, F is the Faraday constant, R the universal gas constant, T is absolute temperature, and Ψ_o is the average potential of the near-surface plane (o-plane) as postulated by the Stern-Grahame modification of the Gouy-Chapman description of the electrical double layer [5]. The equilibrium constants, K_1 and K_2 , can be evaluated using surface titration experiments from which the surface charge can be calculated as a function of pH. An example of surface complexation of divalent metal cations, Me^{2+} , is:



where K_3 can be evaluated from adsorption isotherm data. Additionally, metal-ligand complexes such as $MeOH^+$ can be adsorbed if present, the distribution of which is also controlled by the pH of the system. An example of $MeOH^+$ complexation in the outer layer, assuming a triple layer model (TLM) description of the double layer, is:



where Ψ_β is the average potential of the outer surface, or β , plane. The TLM approach assumes several adsorption planes within the electrical double layer and, therefore, can consider more strongly adsorbed *inner layer* complexes as well as more weakly interacting *outer layer* complexes that resemble ion pairs (e.g., Eqs. (3) and (4)). With this distinction, the model can also include the ion pair-like interactions of the background electrolyte ions with the surface of the solid and thereby capture ion strength effects, a provision not available in some other surface complexation models such as the constant capacitance model. The relevant Electrolyte Surface Reactions involving $NaClO_4$ are presented in Table 1.

The modeling approach used here does not distinguish the various mineral oxide sites according to their base mineral, but regards the total available surface as a single, surrogate surface oxide. A detailed study of potentiometric titration data for glauconite that included dissolution and ion exchange interactions revealed that the *single-site* approach works well owing to the predominance of the surface protolysis species. Figure 1 depicts zinc adsorption edges and TLM simulations for 0.01 and 0.001 M ionic backgrounds. The ionic strength effect is negligible for these conditions suggesting relatively strong interactions between the metal and the surface, characteristic of inner sphere complexes. Triple layer simulations considering only inner layer complexes with free Zn^{2+} did not provide a suitable description of the data for either case. The fit was improved by including outer layer complexes of $ZnOH^+$. This result is compatible with $Zn(II)$ speciation in that Zn^{2+} and $ZnOH^+$ are the species of interest at $pH < 8$, after which precipitation appears to become a significant contributor to metal removal.

Similar to Zn and as presented in Table 1, a set of reactions including inner complexes with Cd^{2+} and outer complexes with $CdOH^+$ yielded the best description of the adsorption edge for $I = 0.01$ $NaClO_4$. Triple layer analysis that includes outer layer complexes of $CdOH^+$ has been postulated in some previous cases of cadmium adsorption onto iron [6-7]. The presence of significant outer sphere complexes may be an indicator of sensitivity of adsorption to the ionic strength of the background electrolyte solution. The ionic background concentration does exhibit some, albeit small, impact on the adsorption edge for cadmium with the largest variations at lower pH values. Cadmium removal onto glauconite decreases for an increase in ionic strength. This pattern has been observed in several other studies of metal adsorption onto nonhomogeneous oxides [6]. For a higher ionic strength of 0.1 M $NaClO_4$, the combination of reactions and associated constants determined at $I = 0.01$ M also provides a good estimate of the adsorption edge. At $I = 0.001$ M, however, the model substantially

underestimates Cd(II) removal at lower pH. Additional simulations revealed that a higher value for the equilibrium constant for the inner layer Cd^{2+} complex improved the fit.

For an ionic background of 0.01 M, a suitable TLM fit was obtained for Pb pH-adsorption edges using inner layer complexes of Pb^{2+} only, and not substantively improved by inclusion of other reactions. The soluble lead speciation diagram suggests that the free metal ion (Pb^{2+}) is the important species to consider at pH values preceding the onset of significant Pb(II) precipitation at about pH 6. The proposed adsorption reaction, therefore, is consistent with this condition.

The relative adsorption affinity of metals onto glauconite is also illustrated in the column results of Figure 2. Complete breakthrough ($C/C_0=1$) was achieved for Cd, Zn, Cu, and Pb at 800, 1200, 3000, and 7000 bed volumes, respectively for an initial solution pH of 5.5. These results also yield insight into the nature of competitive interactions between heavy metals and glauconite. In the initial stage of the experiment when there is an excess of surface, the solutes compete for available sites and the metals having stronger binding affinities (*i.e.*, Pb and Cu) compete more effectively with preferential removal from solution. As the run progresses and the available surface sites for binding Cd and Zn are saturated, however, Pb and Cu not only react with the remaining sites, but also displace a portion of the weakly-bound Cd and Zn, resulting in C/C_0 values greater than 1.

Figure 3 depicts column breakthrough data for a single solute Zn solution using NR-1 sorbent. Overall adsorption capacity for Zn was similar to that obtained by glauconite. As indicated from batch rate tests and in the slow continuous removal of Zn above 1500 bed volumes in Figure 3, the sorption rate is less rapid for both NR-1 and NR-2.

Continuing investigations are focussing on applications considerations such as multicomponent interactions, effects of metal complexing agents, the stability of the minerals under aerobic conditions, and sorbent regeneration and disposal. Further studies on the contributions of multi-site adsorption, cationic exchange with (for example) potassium, and mineral dissolution to metal uptake and modeling of these phenomena are also in view

- The authors acknowledge the support of Texas Advanced Technology Program under Grant No. 3613006 for this study.

References

1. Smith, E.H.; Lu, W.; Vengris, T.; Binkiene, R. *Wat. Res.* **1996**, 30(12), 2883-2892.
2. Lu, W.; Smith, E.H. *Geochim. et Cosmochim. Acta* **1996**, 60(18), 3363-3373.
3. Newman, A. C. D.; Brown, G. The chemical constitution of clays. In *Chemistry of clays and clay minerals* (ed. A. C. D. Newman, ed.). Wiley: New York, 1987; pp 1-128.
4. Deer, W. A.; Howie, R. A.; Zussman, J. *An Introduction to the rock-forming minerals*. 14'th impression. Longman, 1983.
5. Schindler, P.W.; Stumm, W. (1987) "The surface chemistry of oxides, hydroxides, and oxide minerals." In *Aquatic Surface Chemistry*, W. Stumm, ed., Wiley: New York.
6. Cowan, C.E.; Zachara, J.M.; Resch, C.T. *Environ. Sci. Technol.* **1991**, 25, 437-446.
7. Benjamin, M.M.; Leckie, J.O. *J. Coll. Int. Sci.* **1981**, 79, 209-221.
8. Baes, C.F.; Mesmer, R.E. *The Hydrolysis of Cations*. Wiley: New York, 1976.

Table 1: Equilibrium Constants for Cd, Pb, and Zn Adsorption by Glauconite Using Triple Layer Model

	<u>pK^c</u>
<i>Surface acidity reactions</i>	
$>\text{XOH} + \text{H}^+ = >\text{XOH}_2^+$	-4.23
$>\text{XOH} = >\text{XO}^- + \text{H}^+$	8.26
<i>Electrolyte surface reactions</i>	
$>\text{XOH} + \text{H}^+ + \text{ClO}_4^- = (>\text{XOH}_2^+ - \text{ClO}_4^-)^0$	-7.45
$>\text{XOH} + \text{Na}^+ = (>\text{XO}^- - \text{Na}^+)^0 + \text{H}^+$	5.03
<i>Cadmium:</i>	
<i>Inner and outer layer surface reactions</i>	
$>\text{XOH} + \text{Cd}^{2+} = >\text{XOCd}^+ + \text{H}^+$	4.26
$>\text{XOH} + \text{Cd}^{2+} + \text{H}_2\text{O} = (>\text{XO}^- - \text{CdOH}^+) + 2\text{H}^+$	8.88
<i>Hydrolysis reactions:</i>	
$\text{Cd}^{2+} + \text{H}_2\text{O} = \text{CdOH}^+ + \text{H}^+$	10.03
$\text{Cd}^{2+} + 2\text{H}_2\text{O} = \text{Cd}(\text{OH})_2 + 2\text{H}^+$	20.35
$\text{Cd}^{2+} + 3\text{H}_2\text{O} = \text{Cd}(\text{OH})_3^- + 3\text{H}^+$	33.30
<i>Lead:</i>	
<i>Inner layer surface reactions</i>	
$>\text{XOH} + \text{Pb}^{2+} = >\text{XOPb}^+ + \text{H}^+$	-3.32
<i>Hydrolysis reactions:</i>	
$\text{Pb}^{2+} + \text{H}_2\text{O} = \text{PbOH}^+ + \text{H}^+$	7.71
$\text{Pb}^{2+} + 2\text{H}_2\text{O} = \text{Pb}(\text{OH})_2 + 2\text{H}^+$	17.12
$\text{Pb}^{2+} + 3\text{H}_2\text{O} = \text{Pb}(\text{OH})_3^- + 3\text{H}^+$	28.06
<i>Zinc:</i>	
<i>Inner and outer layer surface reactions</i>	
$>\text{XOH} + \text{Zn}^{2+} = >\text{XOZn}^+ + \text{H}^+$	1.58
$>\text{XOH} + \text{Zn}^{2+} + \text{H}_2\text{O} = (\text{XO}^- - \text{ZnOH}^+) + 2\text{H}^+$	7.53
<i>Hydrolysis reactions:</i>	
$\text{Zn}^{2+} + \text{H}_2\text{O} = \text{ZnOH}^+ + \text{H}^+$	9.0
$\text{Zn}^{2+} + 2\text{H}_2\text{O} = \text{Zn}(\text{OH})_2 + 2\text{H}^+$	17.9
$\text{Zn}^{2+} + 3\text{H}_2\text{O} = \text{Zn}(\text{OH})_3^- + 3\text{H}^+$	28.4

^c K from mass law for given reaction. Constants for hydrolysis reactions are from reference [8].

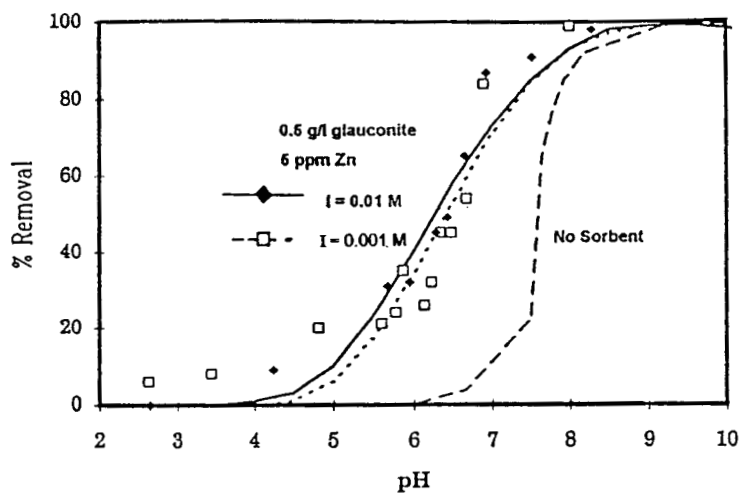


FIGURE 1. Zn - glauconite pH adsorption edge.

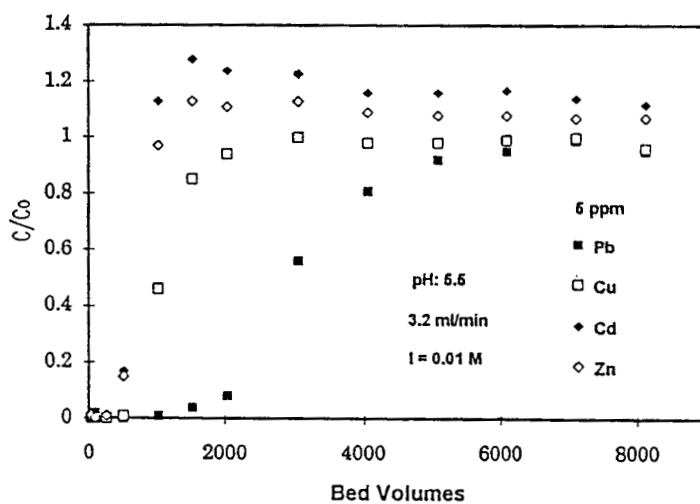


FIGURE 2. Multicomponent breakthrough curves for 60/80 mesh glauconite column.

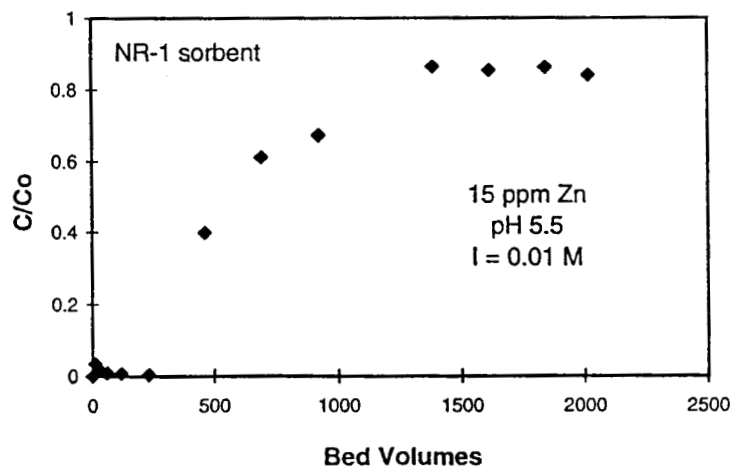


FIGURE 3. Zn breakthrough curve for granular NR-1 sorbent column.